

Scientific Justification for the ALMA Enhancements

ALMA Scientific Advisory Committee

October 15, 2001

Executive Summary

The science cases for the enhancements in the 3-way ALMA project with respect to the baseline 2-way project are presented. The main arguments for equipping ALMA eventually with all 10 receiver bands are: (i) continuous coverage of the main CO and [C II] lines with redshift for both cold and warm gas; (ii) dust emission over a wide range of frequencies to determine dust properties and - for high redshift galaxies - photometric redshifts; (iii) ability to probe gas with a wide range of physical conditions, with temperatures ranging from less than 10 K up to 2000 K and densities up to 10^9 cm^{-3} ; (iv) astrochemistry; and (v) ultimate spatial resolution. The Second Generation Correlator will provide a much higher spectral resolution over the largest bandwidth, which is important for high-redshift CO searches and local molecular line surveys. It will also result in a more flexible use of the available bandwidth, increasing the observing efficiency by at least 9% for all programs and up to a factor of two for some important projects. The case for the Atacama Compact Array (ACA) is driven by the need to recover smooth extended emission that may be missed by the main ALMA array and which will limit the dynamic range of the maps. Without the ACA, not only quantitatively, but also qualitatively wrong conclusions may be reached for some science cases.

Because of the strong science cases for all enhancements and because ALMA has to serve a broad and diverse community, the ASAC has proceeded reluctantly with the request by the E-ACC to prioritize the enhancements. The following ranking has been unanimously agreed upon by the ASAC and is based primarily on scientific merit: 1. *Top priority*: Band 10 and the ACA; 2. *Very high priority*: Band 1 and the Second Generation Correlator; 3. *High priority*: Band 4 and Band 8; 4. *Medium priority*: Band 2 and Band 5. Within each group of two, the rankings are equal, and categories 1–3 are close in absolute ranking.

I. Introduction

At its meetings in Tokyo in April 2001 and Garching in June 2001, the E-ACC requested from the ASAC a presentation of the science cases for the enhancements with respect to the baseline 2-way project made possible by the prospect of the joining of Japan. The E-ACC also requested a prioritization of these enhancements. In the following, a brief written summary of the scientific justification for these components is given, prepared by members of the ASAC with input from technical working groups. The general scientific background is contained in the recent proposal for ALMA Phase II funding submitted to the ESO council in December 2000, and in similar cases submitted to the other agencies.

This document starts with a general introduction on the ALMA receiver bands (§II), followed by the science cases for Bands 1, 4, 8 and 10 (§III–VI), the Second Generation Correlator (§VII), and the Atacama Compact Array (§VIII). The prioritization of the enhancements is contained in §IX.

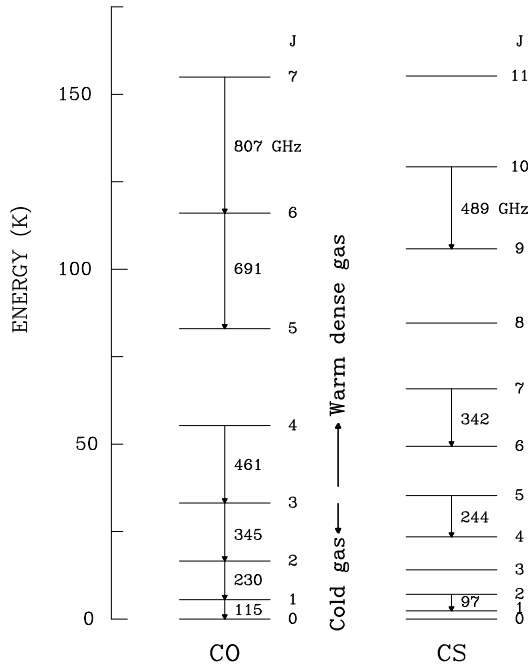


Figure 1. Energy level structure of the CO and CS molecules.

II. The ALMA Receiver Bands

The atmospheric windows accessible to ALMA from the Chajnantor site range from 10 mm (31.3 GHz) to 0.35 mm (950 GHz), and can be covered in 10 frequency bands (see Table 1). The ASAC has stated from the start of the project that ALMA should eventually be equipped with all 10 frequency bands. This desire is driven by various arguments. First, consider the energy level structure of the dominant molecule to be observed with ALMA, CO (Figure 1). This molecule has the strongest lines in galactic and extragalactic regions and is therefore the prime tracer of molecular gas. The lowest-lying rotational transitions $J=1-0$, $2-1$ and $3-2$ occur in the lower frequency atmospheric windows, and Bands 3, 6 and 7 in the Baseline project have been chosen to cover them. These lines can be excited in low-density ($< 10^3 \text{ cm}^{-3}$), cold ($< 30 \text{ K}$) quiescent gas.

Because star formation and other energetic sources can heat the gas to much higher temperatures, ALMA also needs to have the ability to probe the warm component. The ASAC has chosen Band 9 for the initial complement of ALMA receivers, since it is the highest frequency band which is technologically ready and which occurs in a window with good atmospheric transparency. This band covers the CO $J=6-5$ transition, sensitive to gas with temperatures of 100 K or more. Other, less abundant molecules can probe temperatures up to 2000 K in selected sources. High frequency observations also measure gas with higher densities, up to 10^9 cm^{-3} , especially if molecules with large dipole moments such as CS are observed.

In distant galaxies, the CO lines are shifted to lower frequencies by a factor $1+z$, where z is the redshift. Thus, the lines can readily shift outside the initial receiver Bands 3, 6, 7 and 9 (see Figure 2). Part of the justification for Bands 1 and 4, and to a lesser extent Band 2, is driven by the need to observe both cold and warm gas in high redshift objects. Another strong line is the $^2P_{3/2}-^2P_{1/2}$ fine-structure line of [C II] at 1.9 THz ($158 \mu\text{m}$). This line cannot be observed with ALMA in galactic objects, but becomes visible at higher redshifts (see Figure 3). This line is the major coolant of neutral low-density gas and a probe of distant massive star formation, with the CO/[C II] ratio sensitive to local conditions.

The continuum emission to be observed with ALMA is dominated by thermal radiation from cold dust. In the (sub)millimeter regime, the emission is usually optically thin and its strength increases

Table 1. Overview of ALMA Frequency Bands^a

Band	Frequency Range (GHz)	Principal drivers
1	31.3–45.0	Sunyaev-Zeldovich imaging clusters, high- z cold CO, free-free/synchrotron/dust
2	67.0–90.0	Deuterated molecules 1–0, high- z cold CO
3	84.0–116	CO 1–0, bulk of low-exc. lines, high- z CO, SiO 86 GHz maser
4	125–163	CO $z \approx 1$, high- z dust SED, [C II] $z = 10 - 14$, astrochemistry
5	163–211	H ₂ O 183 GHz, H ₂ ¹⁸ O 208 GHz, [C II] $z = 8 - 10$
6	211–275	CO 2–1, bulk of med-exc. lines, dust SED, high- z CO + dust search, [C II] $z = 6 - 8$
7	275–370	CO 3–2, bulk of med-exc. lines, dust maps, polarization, high- z dust search, [C II] $z = 4 - 6$
8	385–500	[C I] 492 GHz, HDO 464 GHz, CO 4–3, [C II] $z = 2.8 - 4$
9	602–720	CO 6–5, high-exc. lines, dust SED, [C II] $z = 1.0 - 1.4$
10	787–950	[C I] 810 GHz, CO 7–6, dust SED, [C II] $z \approx 1$

^a Bands 3, 6, 7 and 9 are included in the ALMA baseline 2-way project.

very strongly with frequency. By observing the dust emission at multiple frequencies, not only the dust mass, but also the dust properties (e.g., whether the dust grains have grown in size) can be determined. This is another strong argument for including both low and high frequency bands in the initial receiver complement, and are drivers for the extreme Bands 1 and 10. The highest frequency dust observations will also give the ultimate spatial resolution of ALMA, making it possible to image the region of terrestrial planet formation in nearby protoplanetary disks.

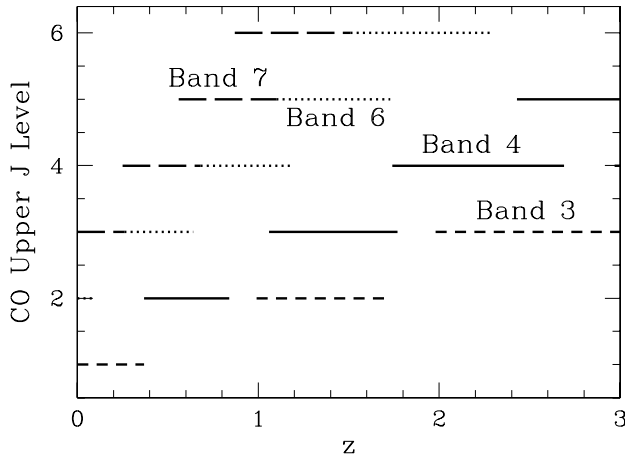


Figure 2. CO lines as a function of redshift z , with the different receiver bands in which they occur indicated (Band 3: short-dashed lines; Band 4: full lines; Band 6: dotted lines; Band 7: long-dashed lines). CO lines with upper level $J \leq 3$ probe cold quiescent gas; those with $J > 3$ warm, dense gas associated with star formation.

Finally, the ALMA receiver bands cover a myriad of molecular lines important for astrochemical studies. The initial Bands 3, 6 and 7 contain thousands of lines of hundreds of molecules and are expected to be the ‘workhorse’ astrochemistry bands, but some species can only be observed at higher frequencies. In particular, light hydrides and the [C I] atom have their fundamental transitions in Bands 8–10.

In summary, the main arguments for equipping ALMA eventually with all 10 receivers bands are: (i) continuous coverage of the main CO and [C II] lines with redshift; (ii) dust emission over a wide range of frequencies to determine dust properties and - for high redshift galaxies - photometric redshifts; (iii) ability to probe gas with a wide range of physical conditions, with temperatures ranging from less than 10 K up to 2000 K; (iv) astrochemistry; and (v) ultimate spatial resolution.

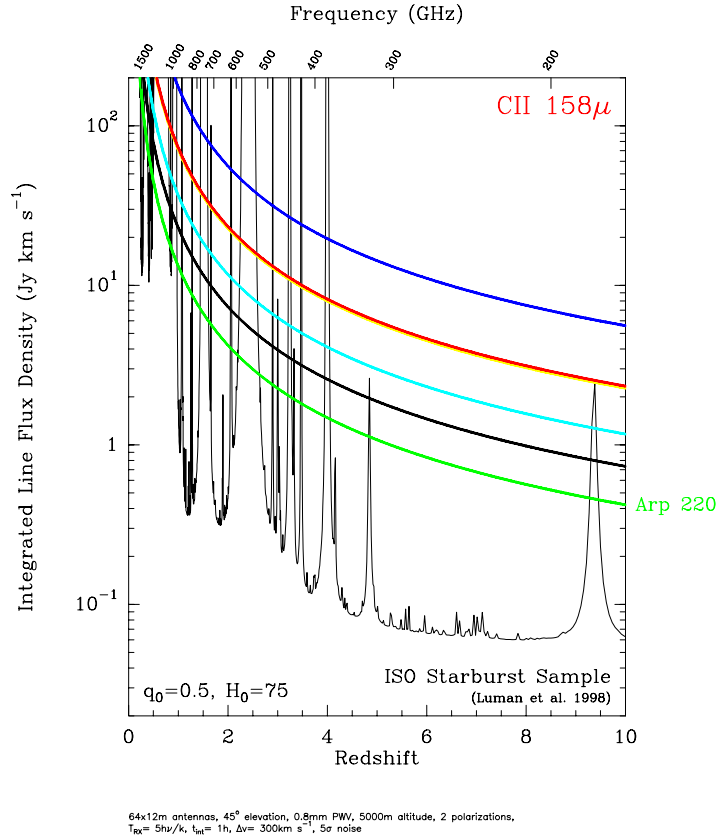


Figure 3. $[C II]$ $158 \mu m$ line intensity as a function of redshift (smooth thick colored lines), compared with the ALMA 5σ sensitivity for 1 hr of integration and a resolution of 300 km s^{-1} (thin line). The structure in the latter reflects the atmospheric features. The different $[C II]$ curves represent extrapolations of the observed $[C II]$ line strengths with ISO in the local starburst sample of Luhman et al. (1998, *ApJ* 504, L11) (Figure by K. Menten).

These arguments are repeatedly found in the individual science cases for Bands 1, 4, 8 and 10 in the following sections. These bands are discussed in order of frequency, not priority, and only their unique scientific capabilities with respect to Bands 3, 6, 7 and 9 in the Baseline project are highlighted.

The lowest priority Bands 2 and 5 (see §IX) are not discussed in detail, but they too contain unique science. Specifically, Band 2 will cover the low-excitation CO 1–0 and 2–1 lines in the redshift ranges $z=0.28\text{--}0.72$ and $1.6\text{--}2.4$, respectively. It also contains the lowest $J=1\text{--}0$ transition of many deuterated molecules, making it possible to study the extreme deuterium fractionation processes found in the coldest gas. Band 5 will be important for red-shifted $[C II]$ lines in the range $z=8\text{--}11$. Moreover, it covers the H_2O 183 GHz and the $H_2^{18}O$ 203 GHz line. The 183 GHz line is a strong maser, but can also probe extended thermal H_2O emission under exceptional conditions. The 203 GHz line offers a unique possibility to image an optically thin isotopic water line from the ground at high angular resolution. Such studies would be important complements to H_2O studies carried out with the Herschel Space Observatory at lower angular resolution in the same timeframe.

III. ALMA Band 1: 31.3–45.0 GHz

ALMA’s lowest frequency Band 1 offers many unique scientific opportunities which no other telescope will be capable of, even by 2010. As well as being a vital adjunct to the main ALMA science programs at higher frequencies, Band 1 would also bring to ALMA an observational community largely distinct from that at (sub)millimeter frequencies. Its observing programs can be carried out even in poor weather. Compared with the upgraded VLA (EVLA), ALMA will be 3.8 times faster at 35 GHz for point-source detection and 17 times faster for wide-field imaging due to its higher aperture efficiency, better site and larger primary beams. Moreover, because ALMA has many short baselines and much better image fidelity, it allows programs not even possible with the EVLA. The key science arguments for Band 1 are as follows.

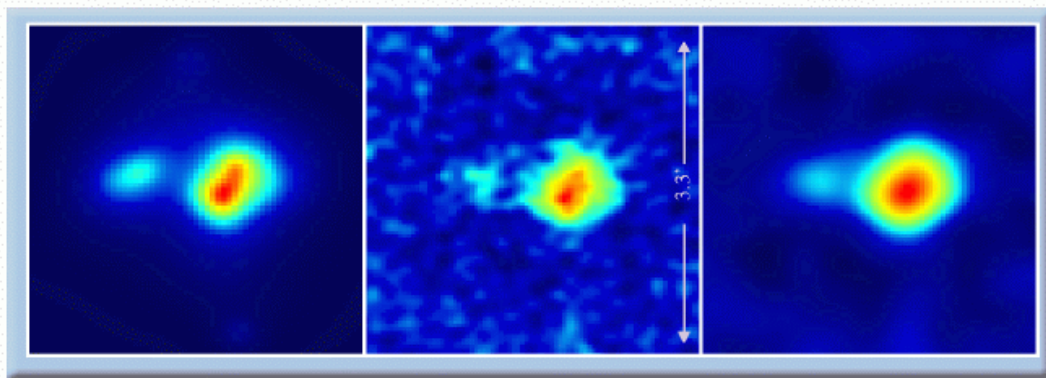


Figure 4. The left panel shows a hydrodynamical model of a $2.5 \times 10^{14} M_{\odot}$ cluster at $z = 1$. The center panel is a 4-hr ALMA image of the cluster at 35 GHz in compact configuration. The rightmost panel shows the same image, smoothed to 22 arcsec (Figure by J. Carlstrom).

1. High-resolution SZ imaging of cluster gas at all redshifts

The Sunyaev-Zeldovich (SZ) effect, in which the cosmic background (CMB) photons are scattered by hot gas in clusters, is independent of redshift and an excellent tracer of cluster mass and physics, especially in combination with new X-ray data provided by Chandra and XMM/Newton. Dedicated SZ surveys from the ground and space will be done over the next few years at lower spatial resolutions of a few arcmin, but ALMA is unique in its ability to map the small-scale structure in cluster gas on tens of arcsec scales (see Fig. 4). Many hundreds of clusters will be detected by these surveys by the end of the decade out to high redshifts, and will be available for ALMA follow-up. The ALMA close-packed array with Band 1 is ideal for this purpose since it contains many short baselines and reaches μK sensitivity in only a few hours.

ALMA will also be important in imaging the very small-scale CMB anisotropies, which occur in the power spectrum at multipoles of $\sim 10,000$. At these scales, theoretical models predict strong CMB fluctuations due to local reionization by early bursts of star formation and due to the effects of massive black hole formation (see Fig. 5). ALMA is the only planned instrument capable of probing the CMB power spectrum on these scales and testing these poorly understood physical processes in the early universe.

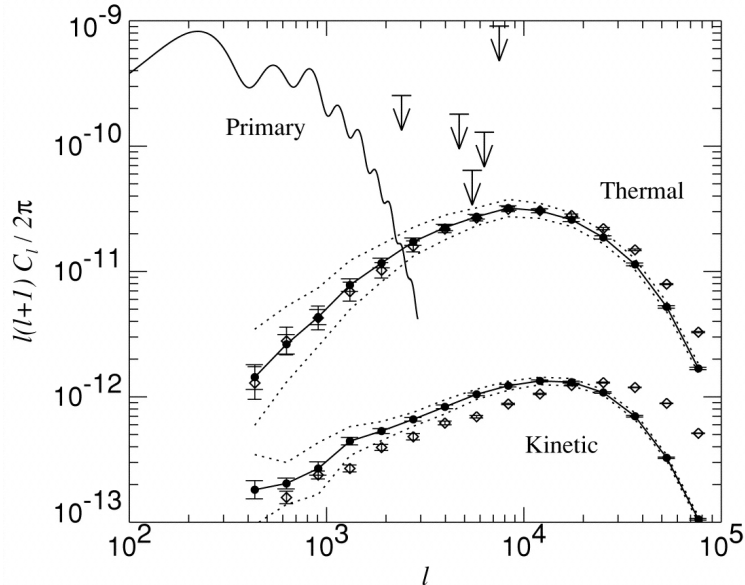


Figure 5. Prediction of the CMB power spectrum on scales of relevance to ALMA by Springel et al. (2001, *Astrophys. J.* 549, 681); a few upper limits from previous experiments are shown. ALMA Band 1 in the close-packed configuration gives many baselines between 15 and 100 m, corresponding to multipoles of 10^4 to 10^5 , right at the predicted peak of the thermal SZ power spectrum. ALMA has sufficient sensitivity to detect these effects, even the kinetic SZ effect, since its sensitivity corresponds to $10^{-12} - 10^{-13}$ in the units plotted on the vertical axis.

2. Mapping the cold ISM at intermediate and high redshift

The reservoirs of gas from which galaxies form may be quite cool, even at moderate redshift z . Most high redshift CO searches to date have focussed on the $J=4-3$, $5-4$ or $6-5$ lines shifted to millimeter wavelengths. Because the CO levels with $J \geq 3$ require densities and temperatures well in excess of what is normally found in average giant molecular clouds, these data preferentially trace the gas associated with dense, actively star-forming regions. The low-lying CO 1-0 and 2-1 lines are the only way to trace very cool gas and measure the kinematics and redshifts of this gas. The recent detection of the 1-0 line in a $z = 3.91$ quasar at 23.4 GHz indicates the presence of a cold halo which is 10-100 times more massive than the gas traced by the higher excitation lines (Papadopoulos et al. 2001, *Nature* 409, 58). Band 1 provides the only means to probe this gas in the CO 1-0 line in the redshift range $z=1.6-2.7$ and in the 2-1 line at $z=4.1-6.3$. It also allows high- z HCN and HCO^+ 1-0 lines to be observed in emission or absorption.

3. Other applications

Other science drivers for Band 1 include (i) Observations of optically thin dust emission from circumstellar disks to probe grain size evolution; (ii) Disentangling the contributions of dust, free-free and synchrotron emission in objects ranging from protostars and supernova remnants in our own Galaxy to starburst galaxies and AGN; and (iii) Searches for the lowest excitation lines of heavy macro-molecules.

IV. ALMA Band 4: 125–163 GHz

ALMA Band 4 covers the range 125–163 GHz (2.4–1.8 mm), where the atmosphere is very transparent even under mediocre conditions. It is a crucial band to measure redshifted CO, [C II] and dust in critical redshift ranges. It also provides important opportunities for astrochemistry.

1. Photometric redshifts and [C II] of the most distant galaxies

In the Band 4 frequency range, the flux densities of high redshift galaxies of a given luminosity do not vary strongly with redshift. With the expected sensitivity, a $4 \times 10^{12} L_{\odot}$ galaxy located anywhere between $z = 1 - 10$ will be detected with $S/N = 10$ in ~ 1 hour in the thermal dust continuum (see Fig. 6). Band 4 is particularly important for the determination of the spectral energy distribution of the highest redshift systems. At $z \sim 10$, the adjacent higher frequency Bands 6 and 7 probe only the peak of the dust spectrum, whereas at the lower frequencies covered by Bands 3 and 1, the emission decreases too steeply to be detectable. To determine the photometric redshift, and eventually also the dust mass and temperature, the turnover frequency of the submillimeter emission needs to be measured, for which ALMA Band 4 is uniquely suited.

Another significant use of Band 4 includes the search for the redshifted [C II] 158 μm emission line in sources with $z=10-14$, the principal cooling line of neutral atomic gas. As Fig. 3 shows, ALMA has the sensitivity to detect this line even at very high redshifts.

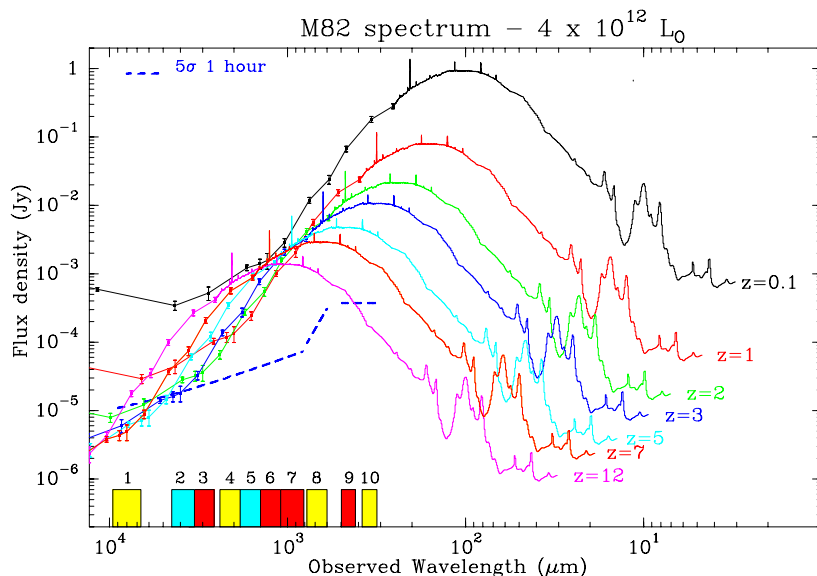


Figure 6. Observer-frame spectrum of a $4 \times 10^{12} L_{\odot}$ galaxy with increasing redshifts from $z=0.3$ to 12. The figure is based on the observed spectrum of M82 including the ISO spectral data and all available radio- and submillimeter data, and assumes a cosmology with $H_o = 50 \text{ km s}^{-1} \text{ Mpc}^{-1}$, $\Omega_0 = 0.3$ and $\Omega_{\Lambda} = 0.7$ (Beelen & Cox 2001, in preparation). The strongest emission line is the [C II] fine-structure line at 158 μm . The positions of the ALMA Bands are shown at the bottom. The thick dashed curves are 5 sigma detection limits after 1 hour of integration time.

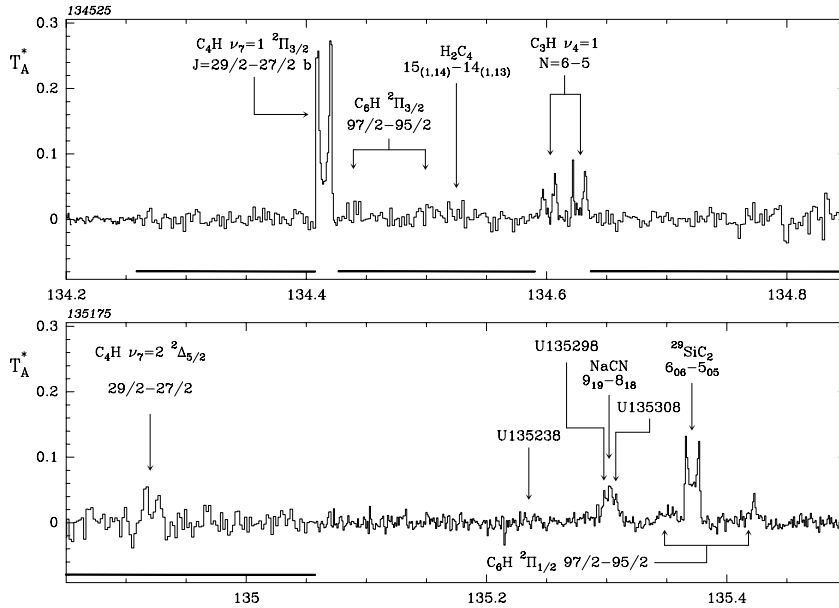


Figure 7. Part of the 2 millimeter spectrum of the carbon-rich AGB star IRC+10216 observed by Cernicharo et al. (2000, *A&AS* 142, 181). Note the many lines from carbon-chain and metal-containing species that can be observed in Band 4.

2. Evolution of normal galaxies up to $z \approx 1$

In normal field galaxies like the Milky Way, most of the molecular gas is in cold ($T \approx 10 - 20$ K) low density gas, in which only the lowest CO $J=1-0$ and $2-1$ lines are significantly excited; observations of local galaxies show that even the $J=3-2$ line is up to a factor of 10 weaker. Band 3 contains redshifted CO $1-0$ and $2-1$ lines in the ranges $z=0.0-0.4$ and $z=1.0-1.8$, but the crucial range $z=0.4-1.0$, during which a strong evolution in star formation is known to have occurred from optical observations, is not covered. Band 4 offers the opportunity to probe the mass, distribution, and kinematics of cold gas in disk galaxies in the critical $z = 0.4 - 0.8$ range (see Fig. 2).

3. Astrochemistry and galactic studies

The Band 4 wavelength range is known to be very rich in spectral lines in star-forming regions and in circumstellar envelopes of AGB stars, and is expected to be a key band for probing the chemistry of circumstellar disks. It contains the $J = 2 - 1$ transition of many simple linear molecules composed of 3 to 4 atoms of cosmically abundant elements, the fundamental transitions of H_2S and NO , important lines of H_2CO , and lines of many linear carbon chain molecules C_nH as well as large organic molecules. In circumstellar envelopes, the conditions are such that the excitation of these heavy molecules peaks in Band 4, so that this will be the prime band to search for rare molecules. Besides carbon-chains, also salts and metal-containing species (AlF , $MgNC$, $NaCN$, ...) and their isotopes can be observed in Band 4 (see Fig. 7), which provide unique probes of the nucleosynthetic history of stars.

Deuterated species in cold clouds are important diagnostics of the temperature evolution of the region, but their lowest $J = 1 - 0$ lines occur in the low-priority Band 2 and are thus not covered. The higher $3-2$ transitions occur in Band 6, but those lines probe only a small fraction of the cold gas. Band 4 covers the $2-1$ lines and is therefore best suited to measure the orders of magnitude enhancements of deuterated species in cold regions.

V. ALMA Band 8: 385–500 GHz

The main scientific drivers for Band 8 are as follows.

1. [C I] fine-structure line in our own and nearby galaxies

The principal driver for Band 8 is the [C I] $^3P_1 - ^3P_0$ ground-state fine-structure line at 492 GHz. This line and the excited [C I] $^3P_2 - ^3P_1$ line at 809 GHz in Band 10 are the *only* fine-structure transitions of an abundant element whose rest frequencies fall in the ALMA range. They probe the transition layer between the atomic medium where most molecules are photodissociated by ultraviolet radiation and the molecular clouds where young stars form. Thus, the [C I] data delineate the surfaces of molecular clouds, and provide vital information on the distribution of the radiation sources as well as the detailed structures of the clouds themselves. Since the star formation rate is likely a sensitive function of the radiation field, ALMA [C I] observations will play a crucial role in improving our understanding in the role of cloud formation and destruction in star formation and galaxy evolution.

Existing single-dish [C I] surveys provide valuable data on the [C I] distribution in galactic clouds (see Fig. 9), but high spatial resolution ALMA data are essential for at least three applications: (i) Nearby galaxies up to $z \approx 0.2$, where ALMA provides comparable resolution to that with single dishes for galactic sources. Recent data (see Fig. 8) show that—in contrast with our own Galaxy—the [C I]/ ^{13}CO ratio is highly variable in different galaxies. ALMA is needed to map the [C I] and ^{13}CO distributions; (ii) Planet-forming disks around young stars in our own Galaxy, which are typically only a few arcsec in extent. Recent studies have shown that the chemistry and thermal balance in the upper layers of disks are controlled by ultraviolet radiation, and [C I] is uniquely suited to trace this; (iii) Physics of galactic clouds, where only ALMA has the spatial resolution to resolve the <1000 AU ($<1''$ at 1 kpc) transition layer and test models. Targets will be edge-on clouds, circumstellar shells and planetary nebulae.

Of the two [C I] lines, the ground-state 492 GHz line is the choice for determining the total column of [C I], whereas the 809 GHz line is needed to constrain its excitation (see Fig. 9 and science case for Band 10). In terms of mapping efficiency, the 492 GHz line will be an order of magnitude faster than the 809 GHz line.

2. Redshifted [C II] fine-structure line at $z = 2.7 - 3.8$

Band 8 covers the red-shifted [C II] $158 \mu\text{m}$ fine-structure line in the important redshift range $z = 2.7 - 3.8$, where much of the star formation and AGN activity is thought to peak. Since [C II] is the dominant cooling line of the neutral atomic gas, it is an important and unique probe of the ‘active’ universe.

3. HDO fundamental transition in solar system objects

The water molecule plays a key role in the astrophysics of star-forming regions as well as solar system objects such as comets. While ALMA cannot observe thermal emission from H_2O itself due to the atmosphere, a substantial fraction of ALMA observing may be devoted to studies of deuterated water, HDO, through its fundamental transition 464 GHz, tracing the thermal history of the cloud. Moreover, the deuterium fraction in comets is critical for an understanding of their origin and plays a large role in discussions on the origin of water on Earth. The ALMA HDO data will complement observations of H_2O with the Herschel Space Observatory to be launched in 2007; this capability should not be much delayed if the same comets are to be observed.

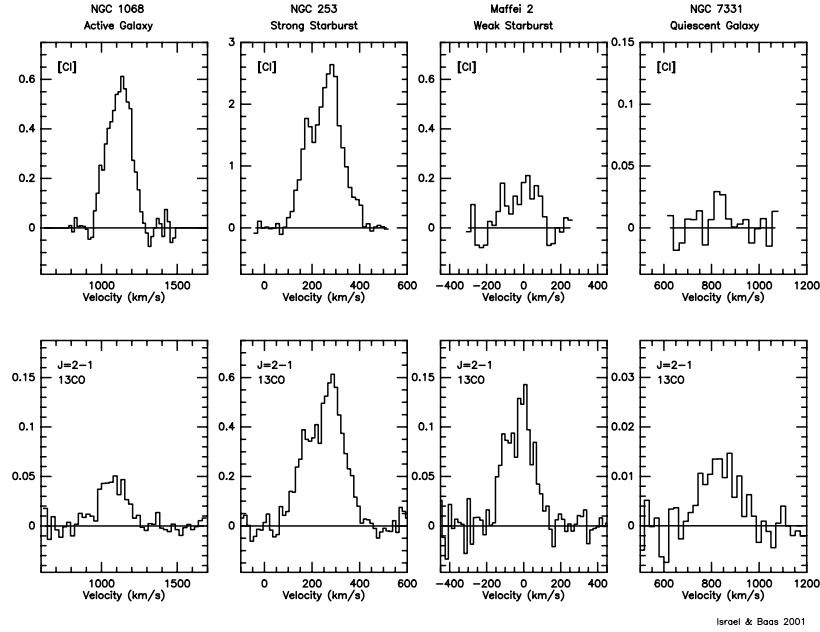


Figure 8. Single-dish $[C\ I]$ 492 GHz and ^{13}CO 2–1 observations of different types of galaxies. Note the different $[C\ I]/^{13}CO$ ratios for active, starburst and quiescent galaxies. ALMA is needed to image the distribution of these species and determine the physical cause for the differences (from Israel & Baas 2001, in preparation).

4. CO $J = 4 - 3$ in our own and local galaxies

In many circumstances, the CO $J=4-3$ line at 460 GHz is the most intense cooling line for warm, dense molecular gas, such as that associated with supernova remnants and outflows from young stars. The COBE results show that for our Galaxy, the $J = 4 - 3$ line is a good measure of the cooling rate in the vicinity of the nucleus. The high spatial resolution of ALMA is needed to resolve shock structures in our own Galaxy (typically few 100 AU, $< 1''$ at 1 kpc) as well as nuclei of external galaxies.

VI. ALMA Band 10: 787–950 GHz

Band 10 is the highest frequency observing band of ALMA, thus providing the highest angular resolution for a given configuration. It offers the following unique science opportunities.

1. Excited [C I] fine structure line

The second $^3P_2 - ^3P_1$ fine structure transition of neutral carbon lies at 809 GHz. This line, along with the lower-lying [C I] $^3P_1 - ^3P_0$ 492 GHz line in Band 8, traces the transition layers between the atomic and molecular gas. Therefore, the [C I] observations provide essential information on cloud structure and evolution in our Galaxy (see Band 8 science case). Whereas the 492 GHz line traces the total [C I] column density, the 809 GHz line is much more sensitive to the gas density and temperature (see Fig. 9). With the high spatial resolution and high sensitivity of ALMA, the detailed distribution of the two [C I] lines can be explored in different types of external galaxies to study cloud formation and destruction on galaxy scales (see also Fig. 8). This is an entirely new field of astrophysics, which can be opened with ALMA for the first time.

2. Red-shifted [C II] emission

Observations of red-shifted atomic lines such as the [C II] 158 μm and [N II] 205 μm lines from distant galaxies are other important targets for Band 10. In particular, Band 10 enables observations of the [C II] emission from galaxies with $z = 1.0 - 1.4$. This redshift range is of interest because of the strong galaxy evolution near $z \sim 1$ (see also case for CO at $z \approx 1$ for Band 4). These [C II] properties and the CO/[C II] ratios at intermediate redshifts $z \sim 1$ must be compared with those at much larger z to be observed in Bands 3–9 corresponding to $z = 2 - 20$.

3. High excitation lines of fundamental molecules

Another important aspect of Band 10 is the rich variety of high excitation lines of fundamental molecules such as HCN $J=9-8$, $10-9$ and HCO⁺ $J=9-8$, $10-9$. For instance, the $J=10-9$ line of HCN has an upper state energy of 230 K, and probes densities of at least 10^8 cm^{-3} . Not only lines in the ground state, but also in excited vibrational states with energies >1000 K can be detected and imaged with the ALMA sensitivity (see Fig. 10). These lines are therefore unique probes of the hottest and densest parts of star-forming regions, protoplanetary disks, and galactic nuclei. Note that the HCN and HCO⁺ $9-8$ lines are the first accessible ones after the $J=4-3$ lines in Band 7, because the $J=5-4$ to $8-7$ lines are significantly blocked by the Earth's atmosphere. Maser emission in the vibrationally excited HCN $J=9-8$ line has also recently been observed toward late-type stars (Schilke et al. 2000, ApJ 528, L37). High spatial resolution ALMA observations of this line will give new insight into the energetic phenomena associated with the mass loss processes of late-type stars. Finally, the CO $J=7-6$ line occurs at 807 GHz, tracing warm (>200 K) and dense gas in both local and more distant objects. This line will serve as a powerful tool to investigate the central regions of starburst galaxies and AGN.

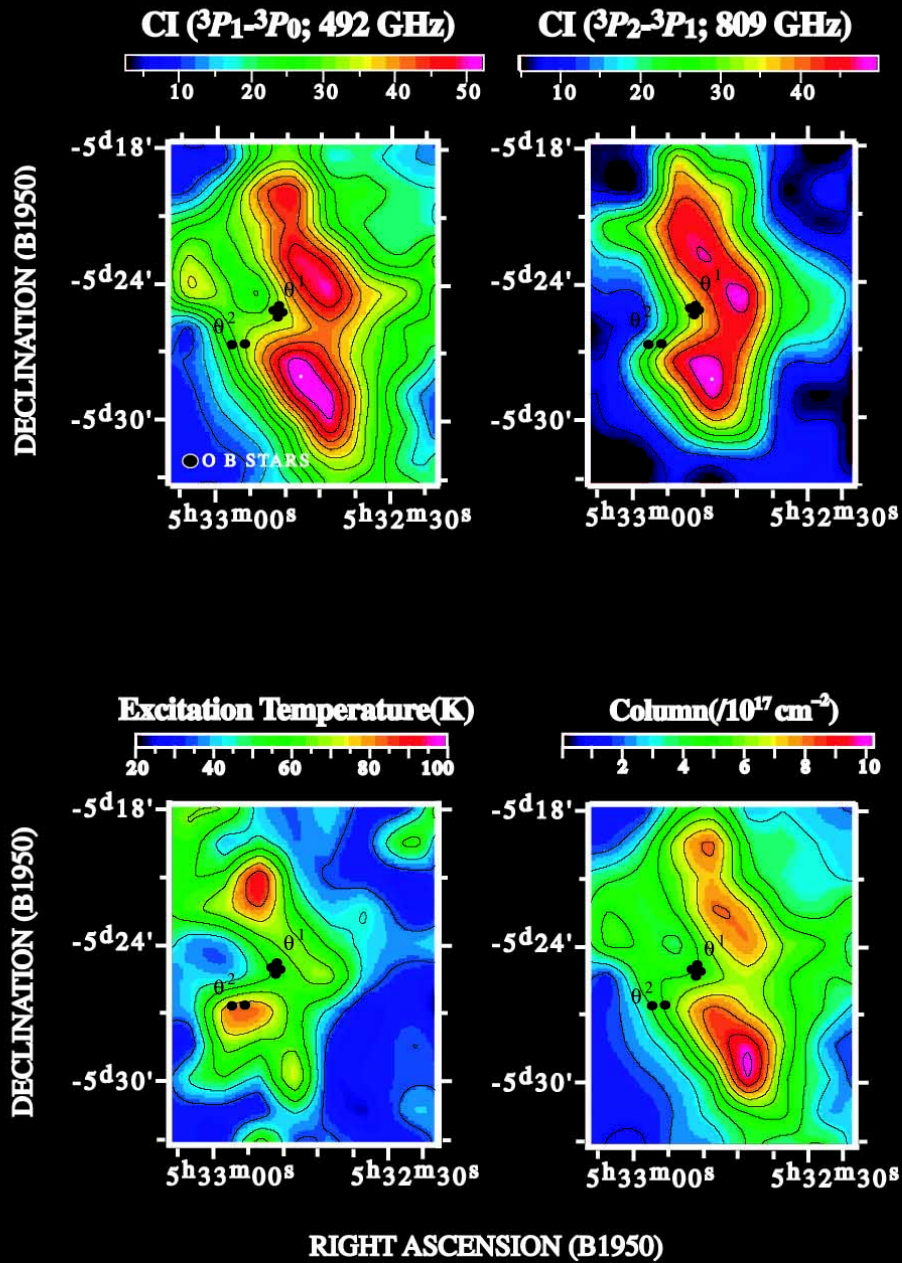


Figure 9. Distributions of the [C I] $^3P_1 - ^3P_0$ (492 GHz) and $^3P_2 - ^3P_1$ (809 GHz) emission around Orion KL observed with the Mount Fuji submillimeter-wave telescope. The 492 GHz line mostly traces the column density, whereas the 809 GHz line is sensitive to the gas temperature (Kuboi et al. 2001, in preparation).

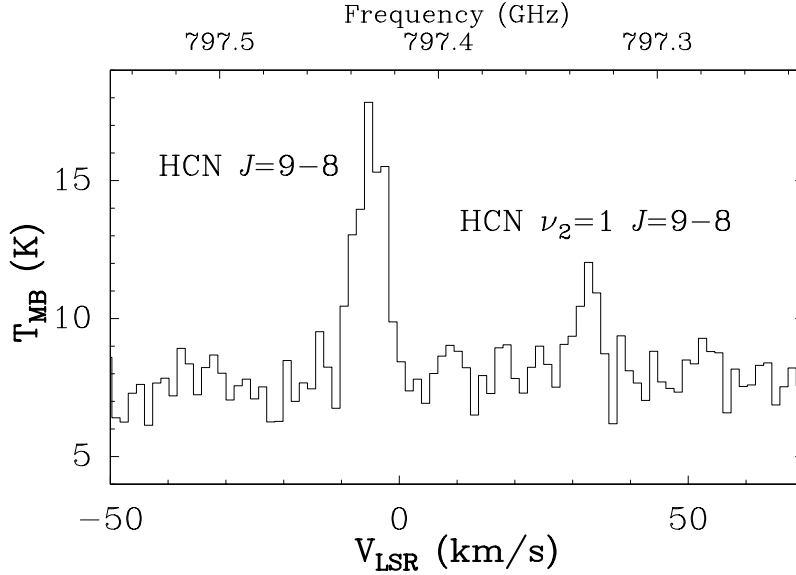


Figure 10. The HCN $J=9-8$ line together with its vibrational satellite observed toward the massive protostar GL 2591. These highly-excited lines probe the conditions of the ‘hot core’ in the inner few hundred AU near the young star, and can be used to trace its evolution (Boonman et al. 2001, *ApJ* 553, L63).

4. Dust continuum emission

Continuum measurements at Band 10 will provide flux information at the highest frequency of ALMA, which will be important for accurate determination of the spectral energy distribution (SED) of objects like protostellar cores, protoplanetary disks, and active galactic nuclei (see also Fig. 6). For example, for protoplanetary disks multi-band photometry is essential to derive both the optical depth and the grain properties, which may give a clue to understanding of grain growth leading to planet formation. Furthermore, the highest angular resolution of ALMA can be achieved with a combination of Band 10 and the longest baselines, which is needed for imaging protoplanetary disks and identifying gaps created by (proto-)planets on scales of 1 AU in the nearest star-forming regions. This high angular resolution at the highest submillimeter frequencies is also important for bridging the gap with (future) ground- and space-based mid-infrared observatories. For distant galaxies, the Band 10 observations can be used together with far-infrared data from SIRTf, ASTRO-F and/or Herschel to determine their bolometric luminosity and photometric redshifts. For $z \approx 5$, the continuum flux will peak in Band 10 (see Fig. 6).

VII. Second Generation Correlator

The Second Generation (2G) Correlator will provide two major improvements to ALMA with respect to the Baseline Correlator: (i) a much higher spectral resolution over the largest bandwidth; and (ii) a highly flexible use of the bandwidth and the telescopes. It can increase the observing speed of some highly ranked programs by a factor of two or more, especially in the areas of high-redshift galaxies and protoplanetary disks around young stars, which require long integration times. At a minimum, the observing efficiency is increased by 9% without any correlator capacity losses. A few science cases are described below.

1. Distant dusty sources

ALMA will be a major instrument in cosmology, in particular in high-angular resolution studies of distant dusty galaxies which optical telescopes cannot probe. The CO lines are the principal redshift indicators and are separated by 115 GHz in the rest frame, and by $115 \text{ GHz} / (1 + z)$ at high redshift, or 19 GHz for $z=5$. Thus, with only a few frequency settings, ALMA will be able to detect at least two lines, as needed to determine z . Such searches will use the maximum bandwidth, primarily in the lower frequency bands, e.g. Band 3. The Baseline Correlator will have a resolution of $\sim 60 \text{ km s}^{-1}$ at 80 GHz over the maximum bandwidth, whereas the proposed 2G Correlator should have $\sim 2 \text{ km s}^{-1}$ under the same conditions. The difference is important because the earliest galaxies are likely to consist of small units with line widths of about 100 km s^{-1} or less, so that such galaxies may only be ‘detected’ in a single channel at 60 km s^{-1} resolution. Not only would this make the detection unreliable, it would preclude any dynamical studies.

The superb point-source sensitivity of ALMA combined with the 2G Correlator also makes it feasible to conduct unbiased spectral surveys of absorption lines toward high-redshift quasars as weak as a few mJy. This capability opens the door to study low excitation molecular gas in intervening clouds and thus probe the missing link between the Lyman- α atomic clouds and galaxies.

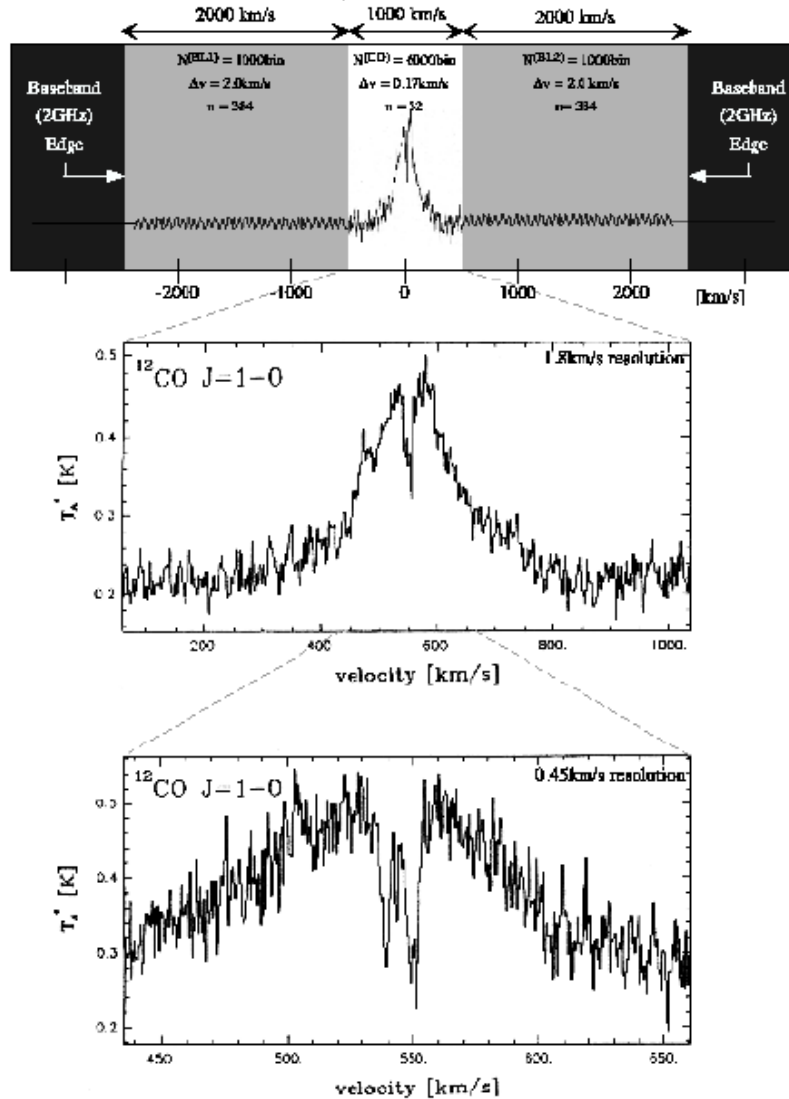
2. Line surveys and searches for pre-biotic molecules

The 2G Correlator with its large bandwidth and high spectral resolution ($< 0.5 \text{ km s}^{-1}$) is also very beneficial for spectral surveys, which provide a wealth of information ranging from an unbiased census of the principal molecules in the sources, to the use of line ratios to constrain their physical structure. With the Baseline Correlator, the required spectral resolution of $< 0.5 \text{ km s}^{-1}$ allows a $\sim 1 \text{ GHz}$ bandwidth at 230 GHz. With the 2G Correlator, this is increased to $\sim 8 \text{ GHz}$, improving the observing speed to cover a full atmospheric window by more than a factor of 10. It gives a spectroscopic capability that parallels that of the modern high-resolution echelle spectrometers that are now standard equipment on leading ground-based optical telescopes.

Unbiased line surveys also offer the opportunity for unexpected discoveries of new species (see Fig. 7). This includes not only exotic molecules, but also pre-biotic molecules such as sugars and amino acids. ALMA will offer many improvements compared with single-dish telescopes because the main targets are small hot molecular cores, where the high ALMA spatial resolution will increase the sensitivity by orders of magnitude and the interferometer will filter out confusing large scale emission. For example, the simplest amino acid conformer glycine II has about 60 transitions in a 16 GHz band around 100 GHz, and its detection requires observations of the largest possible number of transitions at $0.1\text{--}0.2 \text{ km s}^{-1}$ resolution to positively identify this species. In colder regions with less confusion such as protoplanetary disks, the lines are narrow ($< 100 \text{ kHz}$) and often spaced by tens of MHz. Here the flexibility of the 2G Correlator will allow more than twice the number of lines to be selected at very high spectral resolution ($< 0.1 \text{ km s}^{-1}$) and imaged

CO(J=1-0) from Central Region of Cen A

(Reference: Eckart et al. 1990 with SEST)



- (i) Strong Continuum from AGN
- (ii) Detailed Structure of GMC (CO emission)
- (iii) CO Absorption feature with very narrow Δv

Figure 11. Example of the flexible use of the 2G Correlator to study the central regions of active galactic nuclei.

simultaneously. Since the integration times for these projects are very long (> 8 hr per setting), the gain in observing speed is substantial.

3. Probing deep into the centers of active galaxies

The central regions of galaxies contain a mixture of quiescent gas clouds with very narrow lines and gas with extremely wild motions due to rapid rotation and explosive outflows (see Fig. 11). Such an environment can be probed accurately only with the high spectral resolution and wide bandwidth delivered by the 2G Correlator.

VIII. The Atacama Compact Array

1. Background

Ever since the conception of the large millimeter array project(s) in the 1980s, the problem of correctly imaging the large scale structure in maps of astronomical objects has been intensely discussed by the various science advisory groups. It is well known that an interferometer consisting of antennas of the same diameter (a so-called ‘homogeneous array’) is very good at high-resolution imaging of structures that are smaller than the primary beam. However, structures on larger scales are missed, even with multiple antenna pointings (a ‘mosaic’), since the antennas cannot be placed together much closer than ~ 1.2 times the dish diameter. Thus, the baselines that are correlated always have a minimum length which is somewhat larger than the dish diameter. For the 12-m ALMA antennas, the minimum baseline length is about 15 m. This problem is therefore called that of the ‘missing short spacings’. Recovering the large structures is important since they may contain a significant fraction of the flux and are therefore crucial for discussions of quantities such as the kinetic energy and momentum in gas motions. Solving this problem is essential if ALMA is to deliver reliable images to both expert and non-expert users.

The solution to these ‘missing short spacings’ is to either add data from a large single-dish telescope or from an array of smaller antennas. Ideally, the diameter of the single-dish telescope should be at least twice as large as that of the interferometer dishes to pick up those structures on spatial scales that are missed by the interferometer. Since it is difficult to build such a large antenna with sufficiently high surface and pointing accuracy needed for observations at high frequencies, the ASAC and its predecessors have rejected this option. From its roots ALMA was designed to recover these spacings through a novel approach, by operating its antennas in both interferometric mode and total power mode (i.e., by not correlating their signals interferometrically). Simulations for the MMA with 8-m primary antennas showed that good imaging at frequencies below 300 GHz could be achieved by specifying antenna performance at certain levels. These specifications were scaled to the ALMA 12-m diameter antennas; they are an integral part of the project.

A goal of ALMA has been operation at frequencies above 300 GHz, which requires more demanding specifications. For ALMA, a compromise was adopted in the baseline project, by using the very best few 12-m antennas in total power (single-dish) mode and adding their data to the interferometer data. Although this procedure can in principle produce accurate images on large scales, even modest pointing errors can result in a considerable degradation of the dynamic range and fidelity of the maps (e.g., Cornwell 1988, A&A 202, 316). In particular, structures on intermediate scales of 6–15 m baselines may be inaccurately reproduced. As pointed out by Ekers (1999, AIP conf. series 180, 321), even though such inaccuracy may have only a small effect on the final images, they result in a low-level background error over the whole image plane which can be significantly larger than the overall calibration error, especially for complex extended maps. Thus, such errors will make the ALMA goal of obtaining flux accuracies of 1–3% difficult to attain. This goal is most difficult to achieve at the highest frequencies.

The ASAC has therefore advocated the alternative option of adding an array of smaller antennas to the main ALMA array as a possible enhancement in the 3-way project. This array of smaller antennas, taken to be 12 dishes of 7-m diameter, is called the Atacama Compact Array (ACA) and its performance has been intensely studied by the ALMA project, in collaboration with the ASAC. The motivation for the choice of number and size of the ACA antennas is given in ALMA memos 339 and 354. The plan is that the ACA will operate together with the four 12-m antennas in total power mode to accurately measure the missing short spacings.

Simulations of the ACA (including calibration errors) have been performed by three independent groups (J. Pety, F. Gueth & S. Guilloteau at IRAM; K.-I. Morita at Nobeyama; M.A. Holdaway at

Table 2. Examples of ALMA programs with potential ACA candidates indicated

Distance	Object	Linear Size	Angular Size (")	Sample ALMA projects	ACA?
$z \approx 5$	Proto galaxies	10 kpc	3	Blind survey of dust, CO, ...	
$z \approx 0.5 - 3$	SZ effect	1 Mpc	200	Imaging of SZ effect to determine H_0	+
$z \approx 0.1 - 3$	Ultraluminous IR galaxies	10 kpc	6	Imaging structures, line ratios	
$z \approx 0.01$	Galaxies at $z = 0.01$	10 kpc	50	Imaging structures, line ratios	+
10 Mpc	AGN tori	1 pc	0.02	Imaging of obscuring torus	
10 Mpc	AGN, starburst centers	1 kpc	20	Structure and kinematics	+
10 Mpc	Nearby spirals	10 kpc	200	Imaging arm/interarm, line ratios	+
100 kpc	GMC in LMC/SMC	50 pc	100	Line ratios (CI/CO), structure	+
8 kpc	Galactic Center	5 pc	100	Mini spiral, continuum, line	+
5 kpc	Hot cores, UC HII	0.05 pc	2	Line surveys, continuum	
1 kpc	SNRs	0.05-0.5 pc	10-100	Continuum profile, line ratios	
1 kpc	Late-type stars	0.02 pc	4	Line surveys, radial profile	
0.1-1 kpc	Cluster-forming cloud cores	0.01-0.1 pc	2-100	Radial profile, polarimetry	+
0.1-1 kpc	Molecular outflows	0.01-0.5 pc	2-1000	Kinematics, cavities, line ratios	+
0.1 kpc	Infalling protostar envelope	5000 AU	50	Radial profile, line ratios	+
0.1 kpc	Protoplanetary disks	400 AU	4	Dust + molecules, gaps, line ratios	
10 pc	Debris disks main-seq. stars	400 AU	40	Structure, gaps	+
	Planets		50	Structure atmosphere, e.g., Jupiter, Mars	+
	Comets		2-100	Jets, distributed molecules in coma	+
	Sun		1800	Limb brightening, solar activity	+

NRAO) (see also the ASAC September 2001 report, ALMA memos 354, 368, 374, 386, 387 and 393, and <http://iram.fr/~alma>). These groups used two different techniques — CLEAN and MEM—, which give similar results. The main conclusion is that the addition of the ACA to the baseline ALMA will improve the reliability of the images and make the results less dependent on pointing and primary beam errors. The fidelity of the images —i.e., the inverse of the relative error— is improved by 30 to 100% by adding the ACA, reaching values of 30–60 expected in typical observing conditions, thereby improving recovery of the smooth extended emission. These conclusions are based on a series of simulations, which were performed on a suite of test images spanning a large range in properties, including different dynamic ranges in both intensity and spatial scales, and various structures such as filaments or compact cores within an extended envelope. Because the assumptions about the single-dish performance are very optimistic in the current simulations, the importance of the ACA will increase if more realistic single-dish errors are adopted.

Another important result is that the addition of the ACA does not increase significantly the complexity of the data processing nor the required computing power. It does, however, add some complexity in the operations, construction and maintenance of ALMA, since the ACA represents another array with a different type of antenna and more receivers, but efforts are made to duplicate as many elements as possible from the main array.

2. Science case

For the 12-m ALMA antennas, the primary beam at the ‘workhorse’ 230 GHz frequency (~ 1 millimeter wavelength) is $27''$ (arcsec), whereas at the highest frequency of 950 GHz it is only $6''$. Table 2 shows a list of high-priority ALMA science projects, with typical linear and angular sizes of the objects. The last column indicates those projects which are likely to benefit from the addition of the ACA data. The ACA is expected to play a particularly important role for projects at high frequencies, where the pointing errors on the 12-meter antennas will be critical ($0.6''$ compared with a $6''$ beam) and where the objects will in general be larger than the primary beam. Typically, $\sim 25\%$ of the projects (in time) are estimated to require the addition of ACA data. Because of its smaller collecting area, the ACA will need ~ 4 times longer integration times than the main ALMA array to reach the required sensitivity. Thus, the ACA will be occupied close to 100% of its time with these projects.

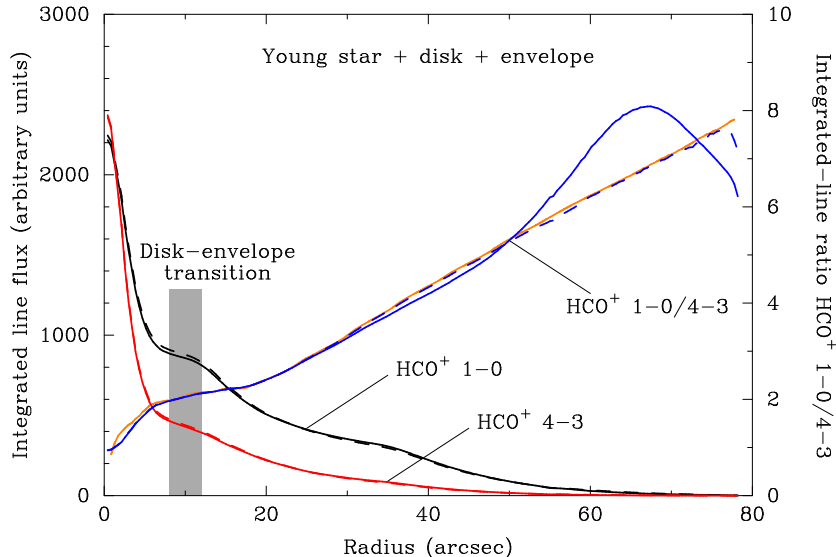


Figure 12. Radial intensity profiles of HCO^+ 1-0 and 4-3 emission (left axis) and HCO^+ 1-0/4-3 line ratio (right axis) in a model of an infalling and rotating envelope and disk around a low-mass protostar. The solid lines show the simulation results with data from ALMA and from 4 12-m telescopes operated in single-dish mode (ALMA + SD); the dashed lines include the ACA data (ALMA + SD + ACA). The line ratio is a measure of the density: the higher the ratio, the lower the density. The light (orange) line is the input model line ratio. The ALMA + SD simulation shows significant deviations from the input model, whereas the ALMA + SD + ACA simulation closely reproduces the model (Figure by M. Hogerheijde).

In order to further justify the importance of the ACA, scientific analyses of the simulation results have been undertaken. This work is in progress and future studies will include a broader range in image properties. The advantages of adding the ACA depend on the source/image structure and content. The effects are sometimes subtle, and may not be readily recognized by non-expert users. In the scientific analysis performed so far, a few examples have demonstrated that, without the ACA, the images will miss key information leading to an inaccurate interpretation of the data. Two salient examples are given below.

Finally, it should be noted that the ACA can also serve as a stand-alone array in a compact configuration at any time for high frequency work. At 900 GHz, the ACA yields an angular resolution of $1.5''$, similar to that provided by the compact configuration of ALMA at 230 GHz. Thus, maps of low- and high-excitation lines could be made with ALMA and the ACA, respectively, and compared on the same angular scale.

3. Two science examples

A. Structure of protostellar envelopes: In the deeply embedded phase of star formation, a protostar is surrounded by a circumstellar disk of size a few hundred AU (a few $''$ at a distance of 100 pc) and a collapsing envelope of size a few thousand AU (up to $1'$). The density structure of the envelope is a key parameter for testing different collapse models and needs to be recovered accurately by the array. Also, the amount of mass transferred from the cloud through the envelope to the disk and finally onto the growing protostar at each stage of evolution is an important question. Figure 12 shows a model of an extended infalling and rotating protostellar envelope for which radiative transfer calculations have been used to generate input images in the $J = 1 \rightarrow 0$ and $4 \rightarrow 3$ transitions of the HCO^+ molecule. The ratio of these transitions is sensitive to the density of

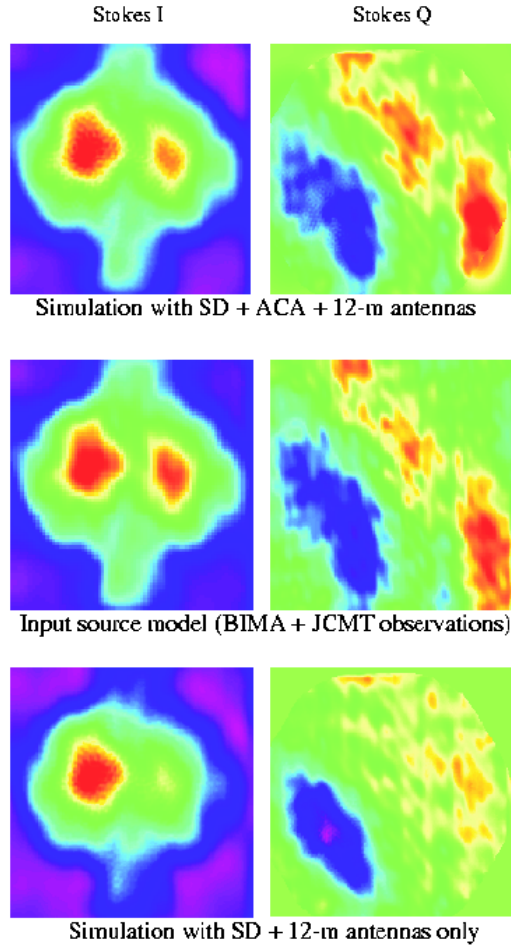


Figure 13. Polarization maps of the Stokes I and Q parameters of the CO 230 GHz line toward Orion OMC1. The input model consists of actual data from the JCMT 15-m telescope combined with BIMA 6-m dish interferometer data (middle panels). Without the ACA (ALMA + single-dish only, bottom panels), the simulations completely fail to reproduce the input image, even for the Stokes I image, with fidelities of only 1–3. For the ALMA + single-dish + ACA simulations (top panels), the fidelities are improved to 10–20 and the structures are correctly reproduced (Figure by R. Crutcher).

the molecular gas and allows one to probe the density structure of the envelope. The (azimuthally-averaged) radial profiles of the $1 \rightarrow 0$ and $4 \rightarrow 3$ lines are shown on the left-hand axis and appear to agree well in the different simulations. However, this is not the case for the density profile of the protostellar envelope, which can only be recovered properly when the ACA is included (Figure 12, right-hand axis). At $2/3$ of the radial extent, the error in the density determination amounts to about 30% when the ACA data information is lacking, leading to an incorrect determination of the radial density distribution. In addition, a qualitatively wrong conclusion that the envelope has an abrupt edge could be reached without the ACA. Adding the ACA, the errors become significantly smaller, only a few %, extending the region over which the density distribution is accurately recovered.

This test image is also representative of the Sunyaev-Zeldovich maps for distant galaxy clusters (see Figure 4), in the sense that there is a strong core surrounded by smooth extended emission. Thus, one can expect improvements by adding the ACA also for this important science case.

B. Polarization: ALMA polarization studies will be able to map polarized emission in molecular clouds, supernova remnants, galaxies, and AGNs. For example, in molecular clouds, ALMA will measure magnetic field morphologies and strengths and be able to answer long-standing questions about the role of magnetic fields in the physics of interstellar turbulence, core formation and support, resolution of the angular momentum problem in star formation, and bipolar outflows. Polarization mapping is probably the most demanding of all ALMA instrumental requirements, for it needs precise measurements of polarized emission that is typically only a few % of the total emission in spite of the fact that instrumental polarization is of the same order.

One science case will be to measure the magnetic field in a turbulent molecular cloud in which cores and protoplanetary disks have formed. Angular scales will range from less than an arcsecond to many arcminutes. Missing polarized flux at zero and short interferometer spacings will lead to a complicated interplay between the partially resolved-out Stokes parameters from more extended structures and those from small-scale structures that will result in polarization maps that are qualitatively, and not just quantitatively, wrong. Indeed, tests made on polarization images of a case of a turbulent molecular cloud (see Fig. 13) show that adding the ACA dramatically improves the recovery of the polarization information. Without the ACA, the fidelities are only 1–3 and the image is not reproduced even qualitatively. Errors on the position angle are of the order of 20° , making it nearly impossible to study the magnetic field morphology. Adding the ACA yields five times smaller errors, i.e. 4° , enabling to recover the polarization information and to study the ratio of turbulent to uniform magnetic field energies, an important parameter in star-formation theories. It is clear that without the ACA and single-antenna polarization data, ALMA's ability to address the crucial question of the origins of stars will be severely handicapped.

IX. Prioritization of the enhancements

The above sections show that there are strong scientific cases for all of the ALMA enhancements. There will be only one ALMA world-wide, and it has to serve a large and diverse scientific community of expert and non-expert users, with interests ranging from distant galaxies to comets in our own solar system. Many of the enhancements, in particular the receiver bands, have been advocated by the ASAC from the start of the project. Certain enhancements are also key features for the Japanese community. It is therefore with considerable reluctance that the ASAC went ahead with the prioritization process requested by the E-ACC.

At the face-to-face meeting in Santiago on September 11–12 2001, the ASAC heard and discussed presentations of the science cases of all enhancements. The ASAC subsequently ranked the enhancements based primarily on scientific merit, with issues such as technical readiness and implementation schedule considered of secondary importance. Nationalistic, political or budgetary factors were not taken into account in the ranking.

The following scientific ranking is unanimously agreed upon by the ASAC. Within each group of two, the rankings are equal. Categories 1–3 are close in absolute ranking.

1. *Top priority*: Band 10 and the ACA
2. *Very high priority*: Band 1 and the Second Generation Correlator
3. *High priority*: Band 4 and Band 8
4. *Medium priority*: Band 2 and Band 5

With the current estimate of the project costs, it is assumed that all enhancements in categories 1–3 can be fitted in the budget for the 3-way project under the “–10% option”, with only the implementation of Bands 2 and 5 deferred to the operational phase. The ASAC requests that it is consulted on further prioritization should budget pressures make it necessary to defer implementation of any of the higher priority enhancements to a later date.